6TH International Conference and Workshop on Engineering and Technology Research (ICWETR) LAUFET 2025: 346-361

Influence of Solar Intensity Fluctuations and Tracking Mechanisms on the Effectiveness of Photovoltaic Solar Systems

[1]Ojelere M. A., [2]Adetola S. O., [3]Sangotayo E. O., and [4]Mudashiru L. O.

[1,2,3,4]Department of Mechanical Engineering, Ladoke Akintola University of Technology, Ogbomoso, Nigeria.

https://www.laujet.com/

LAUFET 2025

Keywords:

Solar photovoltaic,
Tracking,
T-test,
ANOVA,
Solar Intensity

Corresponding Author:
eosangotayo@lautech.edu.ng

ABSTRACT

The efficacy of photovoltaic (PV) solar systems is markedly affected by variations in solar intensity and the deployment of tracking devices. This research examined the influence of these elements on the efficacy of photovoltaic systems, highlighting the necessity of maximizing energy capture to improve sustainable energy solutions. The system comprises photovoltaic panels, light-dependent resistors (LDRs), and relay modules that engage tracking actuators based on sensor feedback. An Arduino Mega 2560 microprocessor analyzes sensor data to modify the panel alignment, utilizing a single-axis tracking system in conjunction with voltage sensors to enhance performance. The tracking system has a rotating gear and a sturdy frame engineered for longevity. The microprocessor utilized real-time sunshine measurements from the LDRs to control movement and dynamically modify the panel orientation. The results indicated that tracking techniques markedly improve solar energy use, greatly augmenting the efficiency of photovoltaic systems for both large-scale and off-grid applications. Statistical evaluations utilizing t-tests and ANOVA at a 95% confidence level demonstrate that the tracking mechanism greatly enhances the voltage output of the photovoltaic systems. The results revealed a p-value of 0.00007460, which is below the 0.05 significance threshold, resulting in the rejection of the null hypothesis (H0). The computed F-value (13.4839) exceeded the critical F-value (3.1599), indicating significant variances in voltage outputs across the different orientations (North, South, West, and East) and the tracking setups. This research emphasizes the essential function of tracking technology in optimizing the efficiency of photovoltaic systems under fluctuating sun intensity circumstances. Future directions may encompass the investigation of multi-axis tracking systems and the advanced integration of artificial intelligence to optimize solar energy capture, to enhance the performance and sustainability of solar energy systems.

INTRODUCTION

The knowledge of photovoltaic (PV) solar system operation and functionality across many environmental contexts has gained importance due to the rapid expansion of the PV solar system as a renewable energy source. The efficacy of photovoltaic solar systems is affected by meteorological conditions, as they directly influence irradiance levels and temperature. Weather-related factors can influence the efficiency of inverters, which convert the direct current (DC) produced by solar panels into usable alternating current (AC) for electrical devices (https://www.sciencedirect.com/science/article/pii/S1351421021002572). To maximize their design, operation, and maintenance, photovoltaic solar systems and inverters must be assessed for the impact of meteorological conditions. This enables scientists, engineers, and decision-makers to formulate strategies that enhance the overall effectiveness of solar energy systems. Photovoltaic solar panels provide energy based on their dimensions,

efficiency, and solar exposure. Photovoltaic solar panels and their positioning are two additional parameters that can influence electric power generation. The intensity of irradiation greatly affects the energy generation of photovoltaic panels (Hellström, 2004).

The DC-to-AC solar power inverter, linked to the AC network to provide electricity to the user, is an essential and efficient component in this system, significantly influencing the reliability of energy processing. Photovoltaic transformers comprise a DC/DC booster transformer and a DC/AC inverter, which are crucial for ensuring the high reliability of the solar energy system to accommodate the demands of national networks (García-Rodríguez *et al*. 2023, Chen and Zhang, 2014). The DC/AC inverter generates AC power with a power factor of 1, which is optimized by the DC/DC converter of the solar array to align with the maximum power point. The power factor is often less than one, with values ranging from 0.7 to 0.9, contingent upon the type of load connected to the system (Serban *et al*. 2019; Meng and Chen, 2020). Heat influences the inverter's power and performance by altering electrical resistance and increasing internal losses in heat transformers, where elevated temperatures can harm inverter components and diminish efficiency. Heat sinks, fans, and liquid cooling systems can assist in cooling transformers to minimize losses and enhance efficiency. Consequently, the maintenance and restoration of the panels should be prioritized to enhance their efficiency and longevity. Solar power plants must use an efficient inverter ventilation system to save energy costs and ensure the reliability of the photovoltaic power plant. The photovoltaic system is designed to evaluate the performance and characteristics of photovoltaic devices, including solar panels and solar cells (Jeykishan *et al*. 2021; Hao *et al*. 2023; Hammadi and Mohammed, 2014).

The electrical efficiency of photovoltaic panels can be considerably affected by temperature. It decreases as the temperature of the solar cells increases. According to Stropnik and Stritih (2016), for each degree increase in the temperature of photovoltaic cells, the electrical efficiency of photovoltaic panels may decrease by 0.4% to 0.65%. Alsheekh *et al*. (2021) found that for each 1°C rise in temperature over 25°C, the electrical efficiency of photovoltaic panels diminishes by 0.08%, leading to a 0.65% reduction in power production. Substantial power losses in photovoltaic systems may also arise from the degrading effects of photovoltaic cells. Kaplani (2012) discussed the detrimental impacts observed in field-aged photovoltaic cells that may result in a reduction of effectiveness. The research assessed the impact of temperature degradation on several components of photovoltaic modules by infrared thermography and digital image processing. This study's findings indicate a correlation between the causes of electrical performance degradation and the effects of that degradation, which were detectable by IR thermography. The efficacy of photovoltaic modules may also be influenced by diminished light conditions. According to Firt*h et al.* (2010), the efficiency of PV modules significantly diminishes in low solar irradiation conditions. The efficiency of photovoltaic cells must be enhanced through proficient heat management. Shittu *et al.* (2019) investigated the feasibility of cooling photovoltaic cells with a flat plate heat pipe. The study indicated that the flat plate heat pipe effectively reduced the temperature of solar cells, enhancing electrical efficiency. The numerical analysis compares the electrical performance of PV-only, PV-thermoelectric, and PV-thermoelectric-heat pipe systems to demonstrate the latter's enhanced efficiency.

Mathew *et al*. (2018) proposed the Wind Driven Optimization (WDO) algorithm as a technique for accurately ascertaining the parameters of a double diode model for solar photovoltaic systems. The study indicated that the WDO method can yield optimal values with reduced errors, hence improving the accuracy and flexibility of photovoltaic system electrical modeling. Sangotayo *et al*. (2018) experimented to determine how photovoltaic

hybrid solar cells affect the electrical efficiency of the solar inverter, ensuring system efficacy. The findings revealed a correlation between solar radiation, temperature, and output voltage. However, when the ambient temperature exceeds 30 ºC, the output voltage decreases. The experiment was done at a location with a wind speed of 0-0.2 m/s and an ambient temperature of 27 ºC to 31 ºC. These photovoltaic modules have an exergy efficiency of 49.30%. The electrical and exergy efficiencies were 5.86% and 42.61%, respectively. Solar photovoltaic module efficiency decreases with increasing solar radiation and ambient temperature due to higher solar cell temperature and irreversibility. Also, the study revealed that current silicon photovoltaic modules underutilize solar energy, thereby aiding in assessing optimal performance and selecting solar panels under certain conditions. This study is aimed at analyzing the influence of solar intensity fluctuations and tracking mechanisms on the voltage output of photovoltaic solar systems.

MATERIALS AND METHODS

System Components and Design

The experimental configuration was developed to examine the impact of solar intensity and a single-axis tracking system on the effectiveness of photovoltaic solar systems in terms of voltage output. The principal elements utilized in the system comprised the following: Photovoltaic (PV) panels are utilized to convert solar energy into electrical power. Light Dependent Resistors (LDRs) function as sensors for sunlight intensity, providing data for monitoring modifications. Relay modules control the operation of the tracking motor based on sensor feedback. The Single-Axis Tracking Mechanism allows for the adjustment of the panel's location by rotational movement due to daily variations in sun intensity. Voltage sensors capture and quantify the voltage output of the photovoltaic system. The Arduino Mega 2560 serves as the microcontroller, processing sensor data and modifying the panel orientation as required, while the GSM Module facilitates remote monitoring and control of the device. The tracking system was designed with a revolving mechanism affixed to a robust frame. This mechanism enables the screen to be effortlessly adjusted to optimize sunlight capture. The microcontroller altered the panel based on real-time solar readings, thereby regulating its movement.

Power and Energy Calculations

The solar power system was analyzed based on energy requirements, solar panel selection, and system efficiency.

Daily Energy Requirement Calculation

The total daily energy consumption was calculated using:

$$Effective\ Energy\ Demand = \frac{\text{Total Energy Consumption}}{System\ Efficiency} \qquad (1)$$

$$Effective\ Energy\ Demand = \frac{940}{0.75} \approx 1253Wh/day$$

The total daily energy consumption of all appliances in the system was found to be 940 Wh/day, requiring a sufficiently robust PV system.

Solar Panel Requirement Calculation

The number of required solar panels was estimated based on the average Peak Sun Hours (PSH) in the test location. The required number of panels is calculated as:

$$Number\ of\ Panels = \frac{Total\ Daily\ Energy\ Consumption}{Solar\ Panel\ Wattage \times PSH} \quad (2)$$

Using standard solar panel wattage of 300W:

$$Number\ of\ Panels = \frac{940}{300 \times 4.5} = 0.7$$

Rounding up, a single 300W panel is sufficient to meet the energy demand under ideal conditions.

Motor Torque Calculation

The motor selection was based on the torque, T required to rotate the panel, calculated as:

$$T = F \times r \quad (3)$$

Where: r = Distance from the pivot point (in m) and Panel weight = 8kg (Chien, 2014), Gravitational acceleration (g) = 9.8 m/s^2, Pivot distance (r) = 0.5m

$T = 78.4 \times 0.5 = 39.2Nm$

a motor with a torque rating of 40Nm was selected.

Battery Selection and Sizing

Battery storage is essential for storing excess energy generated during peak sunlight hours and providing power when solar intensity is low or unavailable. The battery selection process considered daily energy consumption, battery voltage, and allowable depth of discharge (DOD) to ensure optimal system performance.

Battery Capacity Calculation

$$\text{Battery Capacity (Ah)} = \frac{\text{Energy Required (Wh)}}{\text{Battery Voltage (V)} \times \text{DOD}} \quad (4)$$

Using a 12V battery system and a DOD of 95%:

$$\text{Battery Capacity (Ah)} = \frac{1253}{12\ X\ 0.95} \approx 100\ \text{Ah}$$

A 12V, 100Ah battery is selected to provide adequate storage capacity with a safety margin for prolonged usage.

Charge Controller Sizing

The charge controller ensures that the battery is charged efficiently without overloading. Its current rating is determined as:

$$\text{Controller Current (A)} = \frac{\text{Panel Power (W)}}{\text{BPanel Voltage}} \quad (5)$$

Using the panel voltage, 34.07 V:

$$\text{Controller Current (A)} = \frac{300}{34.07} \approx 8.8\ \text{A}$$

A 20A charge controller is selected to handle the maximum current with an additional margin.

Design of the Solar Tracking Mechanism

The single-axis solar tracking system was developed to facilitate rotational movement in a single direction daily. The frame was fabricated from mild steel to ensure durability while facilitating ease of movement.

Structural Design

Panel Mounting Frame: The panel was mounted on a rotational basis to enable movement along a single axis. Figure 1 presents an exploded diagram of the smart off-grid solar tracking and power management systems and Figure 2. displays the dimension of the smart off-grid solar tracking and power management systems. A DC motor with a torque rating of 40 Nm was chosen to facilitate the rotation and placement of Four LDRs strategically positioned at the corners of the screen to monitor light intensity from various directions.

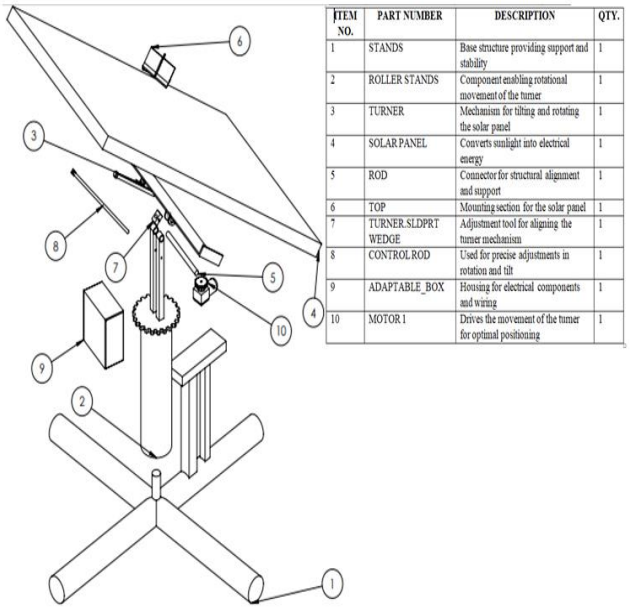

ITEM NO.	PART NUMBER	DESCRIPTION	QTY.
1	STANDS	Base structure providing support and stability	1
2	ROLLER STANDS	Component enabling rotational movement of the turner	1
3	TURNER	Mechanism for tilting and rotating the solar panel	1
4	SOLAR PANEL	Converts sunlight into electrical energy	1
5	ROD	Connector for structural alignment and support	1
6	TOP	Mounting section for the solar panel	1
7	TURNER.SLDPRT WEDGE	Adjustment tool for aligning the turner mechanism	1
8	CONTROL ROD	Used for precise adjustments in rotation and tilt	1
9	ADAPTABLE_BOX	Housing for electrical components and wiring	1
10	MOTOR 1	Drives the movement of the turner for optimal positioning	1

Figure 1: Exploded Diagram of the Smart Off-Grid Solar Tracking and Power Management Systems

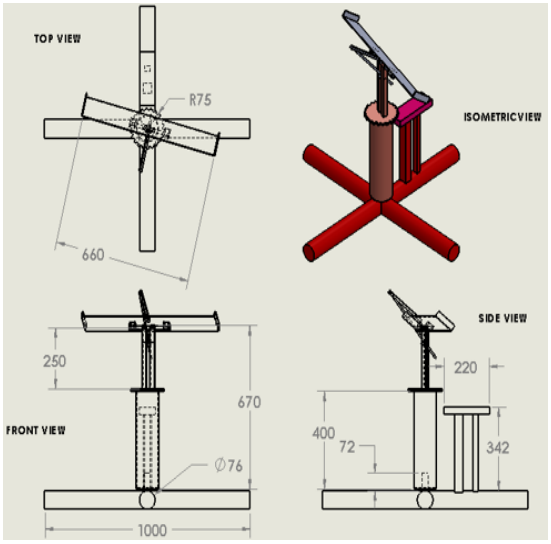

Figure 2: Dimension of the Smart Off-Grid Solar Tracking and Power Management Systems

Experimental Setup and Data Collection

The experiment involved studying voltage generation under varying tracking and fixed-panel circumstances. The methods used include:

1. **Directional Testing:** The photovoltaic panel was manually oriented to face a different cardinal direction each day (east, west, north, and south) without tracking mechanisms.
2. **Single-Axis Tracking Implementation:** Following testing in each fixed orientation, the tracking system was engaged to dynamically modify the panel's position for maximal solar capture.
3. **Voltage Measurement:** Voltage output readings were recorded hourly from 10:00 AM to 6:00 PM for both fixed and tracked configurations.
4. **Solar Intensity Monitoring**: A pyranometer was employed to measure solar radiation levels for comparison with voltage outputs.
5. **Data Logging and Analysis:** Measurements were recorded in a data acquisition system for subsequent analysis, evaluating the efficiency of various orientations in comparison to the single-axis tracking system.

Solar Tracking Mechanism Implementation

The single-axis tracking system was developed to enhance solar panel alignment following the conclusion of fixed-direction testing. The system operated in the following manner:

a) **Daily Rotational Testing:** The panel was oriented in a distinct fixed direction each day (east, west, north, and south) before initiating tracking.

b) **Sun Tracking Activation**: Following fixed-direction assessments, the tracking system was activated to perpetually rotate the panel throughout the day by real-time sunshine intensity sensed by LDR sensors. The tracking motor was regulated by relay modules, which responded to LDR readings to optimize the panel's alignment with maximum sunshine exposure.

c) **Reset Mechanism:** After each day, the panel reverted to its initial position, and prepared for the subsequent testing cycle.

Control Algorithm Development

The control algorithm was designed to synchronize the solar tracking mechanism with the LDR input, guaranteeing optimal sunlight capture during the day. The algorithm was executed on an Arduino Mega 2560 microcontroller, which analyzed real-time light intensity data from four LDR sensors and altered the panel orientation accordingly.

Tracking Logic Implementation

The logic control technique was developed to synchronize the tracking mechanism with the LDR input. The program guaranteed the panel consistently aligned with the sun by assessing light intensity on each sensor and modifying motor movements accordingly. Enhanced capability was incorporated to revert the panel to its initial position at sunset. The microprocessor modified the solar panel's orientation according to the variance in LDR readings:

$$\Delta I = I_{ldr.left} - I_{ldr.right} \tag{6}$$

If ΔI > Threshold, the motor moves in the corresponding direction.

Circuit Diagram Design

The circuit diagram was developed to incorporate the sun-tracking mechanism, power system, and remote monitoring capabilities. The principal linkages comprised:

1. Solar Panel to Charge Controller manages power transmission to the battery.
2. Microcontroller (Arduino Mega 2560) analyzes LDR inputs and regulates motor operations.
3. The Relay Module initiates motor rotation in response to sensor feedback.
4. GSM Module (SIM800L) facilitates real-time remote surveillance and system management.
5. Voltage Regulators guarantee a consistent power supply to all components.

Data analysis

The t-test and analysis of variance were employed. ANOVA, a technique included in the Statistical Analysis System (SAS), applies a series of associated estimation methods to analyze the differences between groups in a sample. One way to conceptualize the test distribution is as a collection of distributions, each with a distinct form dictated by the number of degrees of freedom it contains.

Formulation of Hypotheses

The Null Hypothesis (H0) of Hypothesis 1 states that there is no significant difference in the fixed Orientation and tracking mechanism results at the 95% confidence limit, whereas the Alternate Hypothesis (H1) states that there is a significant difference in the fixed Orientation and tracking mechanism results at the 95% confidence level. To corroborate the findings, the hypotheses were verified using the Analysis of Variance (ANOVA) and t-test with a 95% confidence level.

T-test Probability Distribution

A t-test is an inferential statistic that is employed to ascertain whether there is a substantial difference between the means of two groups and their relationship. A popular statistical instrument used to test differences between the means (averages) of two groups or the difference between one group's mean and a standard value is the t-test, also known as the t-statistic or t-distribution. The Type I error rate may be influenced by unequal variances. Levene's Test of Equality of Variances can be employed to verify the assumption of homogeneity of variance. H0: Null Hypothesis: u1-u2 = 0, where u1 is the mean of the first population and u_2 is the mean of the second population. The formula (7) is employed to calculate the t-test statistic.

$$t = \frac{(\bar{x}_1 - \bar{x}_2)}{\sqrt{\left(\frac{s_p^2}{n_1} + \frac{s_p^2}{n_2}\right)}} \tag{7}$$

where x_1 and x_2 are the means of two groups, n_1 and n_2 are the two groups' samples, and s_p is the population's standard deviation.

Overview of Analysis of Variance (ANOVA) test

One-way analysis of variance (ANOVA) and two-way analysis of variance are the two subcategories of analysis of variance (ANOVA). ANOVA is used to determine whether there are statistically significant differences between the means of three or more independent groups and it is useful when evaluating at least three variables. However, it produces fewer type I errors and applies to a variety of problems. ANOVA classifies differences by

comparing the means of each group and involves distributing variance across multiple sources. Statistical Analysis Software (SAS) was used to compute the statistical measures of variation and aid in making better decisions, such as ANOVA.

Overview of Analysis of Variance (ANOVA) test

One-way analysis of variance (ANOVA) and two-way analysis of variance are the two subcategories of analysis of variance (ANOVA). The One-Way ANOVA evaluates whether or not the three groups differ on a dependent variable and includes one factor, as shown in Table 1, while Table 2 presents a Two-Way Analysis of Variance.

Table 1. One–way ANOVA Distribution

Source of variation	A sum of Squares (SS)	Degree of freedom (df.)	Mean Square (MS)	F-ratio
Between Samples	SSC	v_1=(k-1)	$MSE = \frac{SSE}{(n-k)}$	$\frac{MSbetween}{MSwithin}$
Within Samples	SSE	v_2= (n-k)	$MSE = \frac{SSC}{(n-1)}$	
Total	SST	(n -1)		

Table 2. Two-Way Analysis of Variance

Source of Variation	Sum of Squares	Degree of freedom	Mean sum of Squares	Ratio of F
Between Samples	SSC	(c-1)	$MSE = \frac{SSC}{(C-1)}$	$\frac{MSC}{MSE}$
Between Rows	SSR	(r-1)	$MSR = \frac{SSR}{(r-1)}$	$\frac{MSR}{MSE}$
Residual or Error	SSE	(c-1) (r-1)	$MSE = \frac{SSE}{(r-1)(c-1)}$	
Total	SST	(n-1)		

Where SST is the sum of squares of variances, SSC is the sum of squares for column samples, SSE is the sum of squares for row samples in rows, MSC is the mean sum of squares between samples, and MSE is the mean sum of squares within samples. The two-way ANOVA test is employed for the data classified into two categories, The analysis of variance for a two-way ANOVA is shown in Table 2, SST is the total sum of squares, SSC is the sum of squares for columns, SSR is the of squares for rows and SSE is the sum of squares due to error as written in Equation (8)

$$SSE = SST - (SSC + SSR) \quad (8)$$

Furthermore, the number of degrees of freedom between columns equals (c-1), the number of degrees of freedom between rows equals (r-1), and the number of degrees of freedom for residual equals (c-1) (r-1), where "c" refers to the number of columns and "r" refers to the number of rows. Table 2 presents a Two-Way Analysis of Variance.

The residual or erroneous sum of squares is the total sum of squares minus the sum of squares between columns minus the sum of squares between rows.

RESULT AND DISCUSSION

The study documented the voltage output of a photovoltaic (PV) system for four fixed orientations: East, West, North, and South, as illustrated in Figures 4 to 10. Figure 4 presents a graphical comparison of voltage measurements for a fixed East direction versus a tracking orientation. The maximum was achieved at around 13 hours for tracking orientation (20 volts) and eastern orientation (18 volts). The graphic illustrates the performance profile features for both fixed east orientation and tracking orientation of the voltage output of a photovoltaic (PV) system, which exhibit a similar trend pattern. The data underwent statistical analysis to determine if a significant difference exists between the voltage output in fixed east orientation and tracking orientation, as illustrated in Table 3. Table 3 presents the t-test for comparison of East fixed orientation and tracking mechanism results at a 95% confidence level. The Table indicates that the calculated t-statistic of 2.7200 exceeds the critical values of 1.7613 and 2.1448 for both one-tailed and two-tailed tests, respectively.

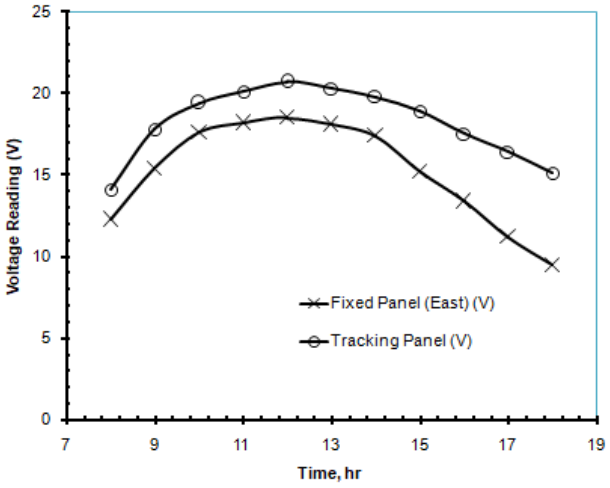

Figure 4: Plot of Voltage reading for Fixed East Orientation and Tracking Orientation

Table 3: t-Test: Two-Sample Assuming Unequal Variances East and Tracking Orientation

	East	*Tracking*
Mean	15.4500	18.6000
Variance	10.0050	3.4067
Observations	10.0000	10.0000
Hypothesized Mean Difference	0.0000	
Df	14.0000	
t Stat	-2.7200	
P(T<=t) one-tail	0.0083	
t Critical one-tail	1.7613	
P(T<=t) two-tail	0.0166	
t Critical two-tail	2.1448	

This indicates a substantial disparity in the East fixed Orientation and tracking method outcomes at a 95% confidence level. Figure 5 presents a graphical comparison of voltage measurements for a fixed South orientation versus a tracking orientation. The apex was achieved at approximately 13 hours for tracking orientation (20 volts) and southern orientation (14 volts). The graphic illustrates the performance profile features for both fixed east orientation and tracking orientation of the voltage output of a photovoltaic (PV) system, which exhibit a similar trend pattern. The results underwent additional statistical testing to determine whether a significant difference exists between the voltage output produced in fixed South orientation and tracking orientation, as illustrated in Table 4. Table 4 indicates that the calculated t-statistic of 5.072601258 exceeds the critical values of 1.734063592 and 2.100922037 for both one-tailed and two-tailed tests, respectively. This indicates a substantial disparity in the outcomes of the South fixed orientation and tracking system at a 95% confidence level. These findings correspond with prior research indicating that single-axis tracking enhances voltage generation by roughly 15–20% relative to stationary systems (Firth *et al*.2010).

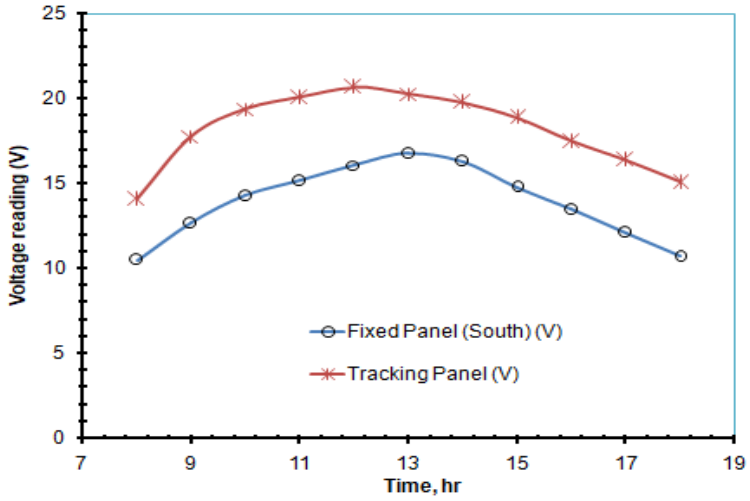

Figure 5: Plot of Voltage reading for fixed South orientation and tracking orientation

Table 4: t-Test: Two-Sample Assuming Unequal Variances South and Tracking Orientation

	South	**Tracking**
Mean	14.25	18.6
Variance	3.947222222	3.406666667
Observations	10	10
Hypothesized Mean Difference	0	
Df	18	
t Stat	-5.072601258	
P(T<=t) one-tail	3.96812E-05	
t Critical one-tail	1.734063592	
P(T<=t) two-tail	7.93625E-05	
t Critical two-tail	2.100922037	

Figure 6 presents a graphical comparison of voltage measurements for a fixed West orientation versus a tracking orientation. The apex was reached at around 12.5 hours for tracking orientation (20 volts) and southern orientation (14 volts). The graphic illustrates the performance profile features for both fixed east orientation and tracking orientation of the voltage output of a photovoltaic (PV) system, which exhibit identical trend patterns. The results underwent additional statistical testing to determine whether a significant difference exists between the voltage output in fixed West orientation and tracking orientation, as illustrated in Table 5. The value of t-stat Calculated, 3.22, is greater than the critical values of 1.734 and 2.100 for both one-tail and two tails, respectively. This suggests that the West fixed orientation and tracking orientation results exhibit a substantial difference at a 95% confidence level.

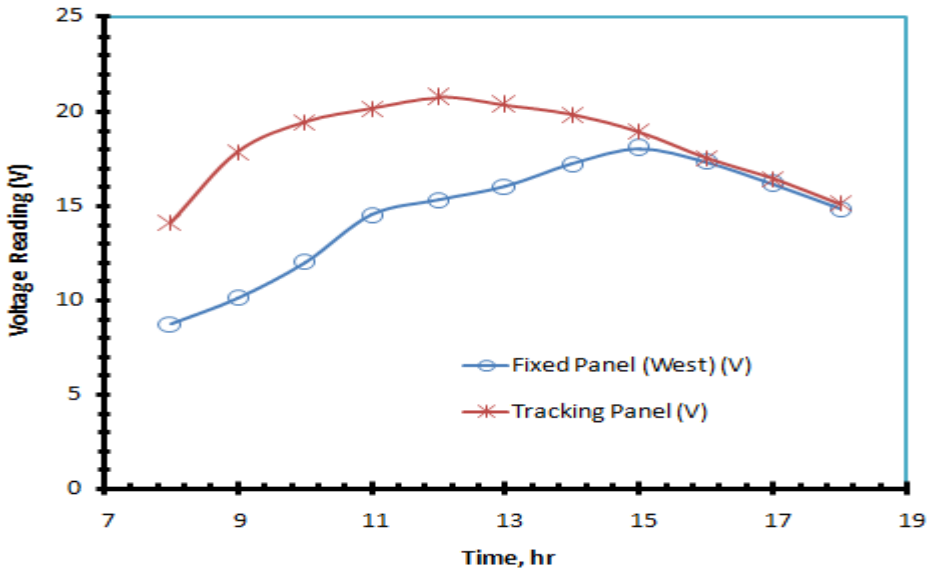

Figure 6: Plot of voltage reading for fixed West orientation and tracking orientation

Table 5: t-Test: Two-Sample Assuming Unequal Variances for West and Tracking Orientation

	West	Tracking
Mean	14.54545455	18.19090909
Variance	9.214727273	4.906909091
Observations	11	11
Hypothesized Mean Difference	0	
df	18	
t Stat	-3.217403412	
P(T<=t) one-tail	0.002388075	
t Critical one-tail	1.734063592	
P(T<=t) two-tail	0.00477615	
t Critical two-tail	2.100922037	

A graphical comparison of voltage measurements for a fixed North orientation and a tracking orientation is illustrated in Figure 7. The apex was achieved at approximately 12.5 hours for the South orientation (12 volts)

and the tracking orientation (20 volts). The performance profile of the voltage output of a photovoltaic (PV) system that exhibits the same trend pattern is illustrated in the Figure for both the fixed east orientation and the tracking orientation. The results were subsequently subjected to statistical tests to determine whether there was a significant difference between the results obtained in the fixed North orientation and the tracking orientation of the voltage output, as illustrated in Table 6. The values of t-stat Calculated, 8.5550, are greater than the critical values of 1.7247 and 2.0859 for both one-tail and two-tail, respectively, as illustrated in Table 6. This suggests that the North fixed orientation and tracking orientation results exhibit a substantial difference at a 95% confidence level.

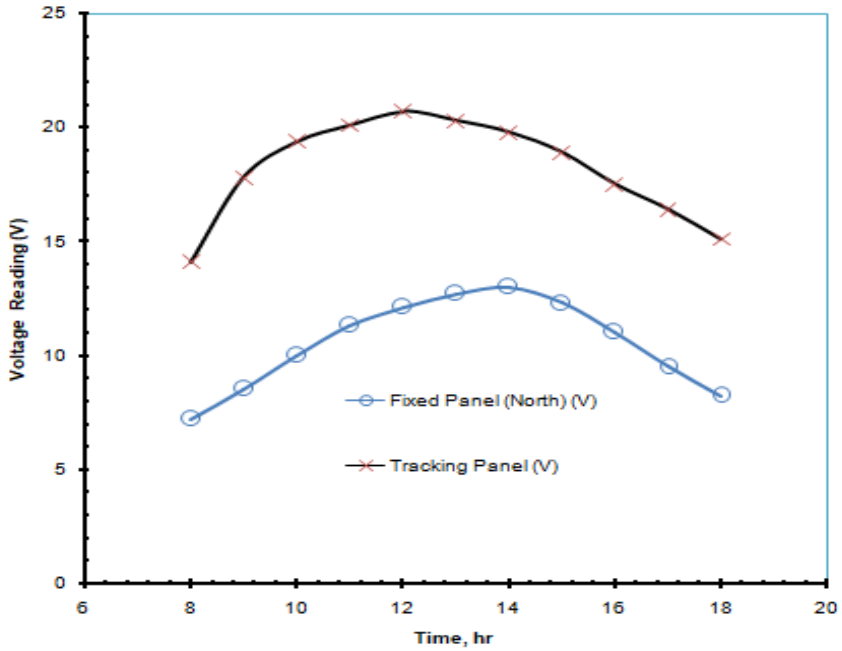

Figure 7: Plot of voltage reading for fixed North orientation and tracking orientation

Table 6: t-Test: Two-Sample Assuming Unequal Variances North tracking Orientation

	North	Tracking
Mean	10.52727273	18.19090909
Variance	3.920181818	4.906909091
Observations	11	11
Hypothesized Mean Difference	0	
Df	20	
t Stat	-8.555047641	
P(T<=t) one-tail	2.03628E-08	
t Critical one-tail	1.724718218	
P(T<=t) two-tail	4.07257E-08	
t Critical two-tail	2.085963441	

Figure 8 illustrates the intensity fluctuations that occur over time for various orientations, including four fixed orientations: East, West, North, and South. The performance profiles of the voltage output of a photovoltaic (PV) system exhibit a consistent trend pattern for all fixed orientations, as illustrated in the Figure. Table 7 presents the ANOVA two-factor without replication for intensity for various orientations at a 5% significance level.

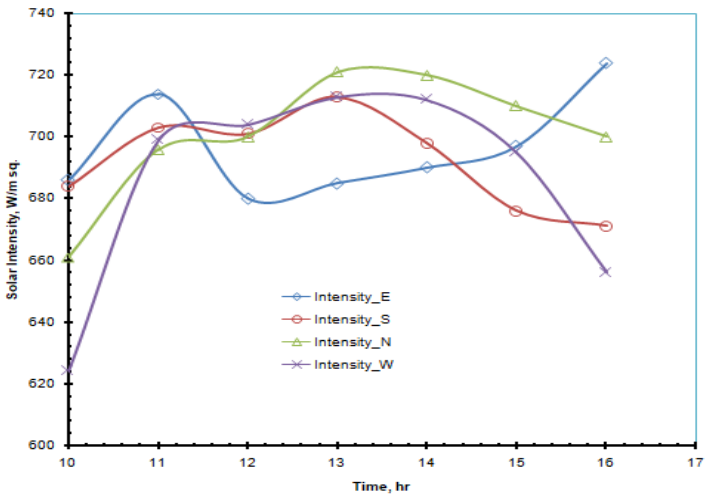

Figure 8: Plot of intensity versus time

Table 7: Anova: Two-Factor Without Replication for Intensity for different orientations

Source of Variation	*SS*	*df*	*MS*	*F*	*P-value*	*F crit*
Rows	5429.714	6	904.9524	2.3880	0.0711	2.6613
Columns	856.1071	3	285.3690	0.7530	0.5348	3.1599
Error	6821.143	18	378.9524			
Total	13106.96	27				

Since the F statistic of 0.7530 is less than the critical F value of 3.1599, the null hypothesis (H0) is accepted, indicating no significant difference in solar intensity across different orientations. Consequently, the alternative hypothesis is rejected, which posits a significant difference in solar intensity for various orientations. Figure 9 illustrates the variations in intensity over time for different orientations, while Table 8 displays the results of a Two-Factor ANOVA without replication under no load at a 95% confidence level. The Orientation, N, S, W, and E variables in the ANOVA are the first to be examined. The p-value is 0.00007460, which is less than the 0.05 (5%) significance level.

The decision rule (Table 8) states that H0 is accepted and H1 is rejected if the computed F value is less than the tabulated F value. The null hypothesis (H0) is rejected because the calculated F (13.4839) is greater than the tabulated F (3.1599). This rejection implies that the orientations N, S, W, and E are not significant. Conversely, the alternative hypothesis (H1) is accepted, which confirms that the voltage results of the orientations N, S, W, and E are significantly different. Table 9 illustrates the Two-Factor ANOVA without replication tracking with load at a 5% significance level, while Figure 10 illustrates the variations in intensity over time for various orientations. The results examined the correlation between voltage output across various orientations and time

intervals, utilizing ANOVA tests, as illustrated in Figure 10 and Table 9. The results indicated that the p-value is 7.45E-17, which is below the 0.05 (5%) significance threshold.

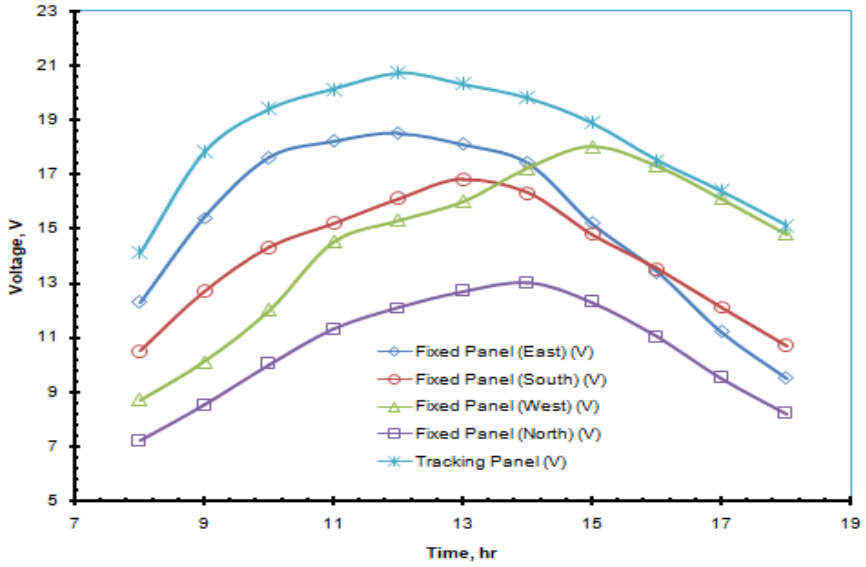

Figure 9: Plot of the effect of tracking on Voltage with no load

Table 8: Anova: Two-Factor Without Replication for Voltage Readings

Source of Variation	*SS*	*df*	*MS*	*F*	*P-value*	*F crit*
Time	1.317142857	6	0.21952	2.1244	0.10068911	2.6613
Orientation, N, S, W, E	4.18	3	1.39333	13.4839	0.00007460	3.1599
Error	1.86	18	0.10333			
Total	7.357142857	27				

The decision rule (Table 9) stipulates that if the computed F value is less than the critical F value, H0 is accepted and H1 is rejected. Given that the computed F value (64.0500) exceeds the critical F value (2.6060), the null hypothesis (H0) is rejected, signifying that the orientations N, S, W, and E are not significant. Consequently, the alternative hypothesis (H1) is accepted, affirming that the fixed orientations (N, S, W, E) and tracking voltage results are significantly disparate. This suggests that fluctuations in voltage output are mostly attributable to the panel's capacity to harness available sunlight, rather than disparities in solar exposure among orientations.

Table 9: Anova: Two-Factor Without Replication Voltage under load condition

Source of Variation	SS	df	MS	F	P-value	F crit
Time	94.29382	10	9.4294	13.5070	5.99E-10	2.0772
Orientation & tracking	178.8556	4	44.7139	64.0500	7.45E-17	2.6060
Error	27.92436	40	0.6981			
Total	301.0738	54				

CONCLUSIONS

This study established that variations in solar intensity substantially influence the effectiveness of photovoltaic (PV) systems and that tracking techniques are essential for maximizing energy capture. The research exhibited a significant enhancement in voltage output through the utilization of a single-axis tracking system governed by an Arduino Mega 2560 microprocessor, as confirmed by statistical analyses applying t-tests and ANOVA. The p-value and the F-value signify substantial changes in voltage output among all orientations and tracking configurations.

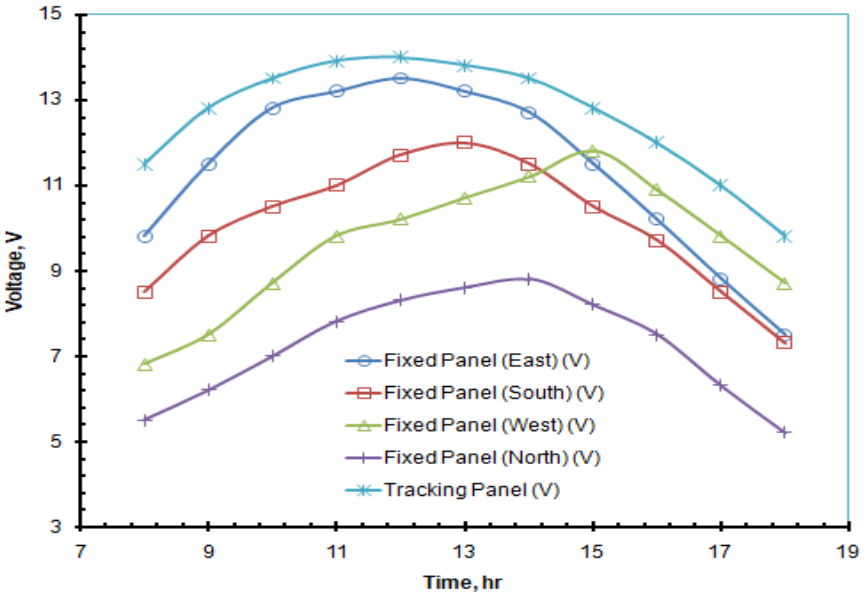

Figure 10: Plot of the effect of tracking on Voltage under load conditions

The results demonstrated the efficacy of real-time sensor-based tracking in optimizing solar energy usage, rendering it a significant method for both large-scale and off-grid photovoltaic applications. The incorporation of light-dependent resistors (LDRs), relay modules, and a resilient mechanical tracking mechanism guarantees enhanced performance and system longevity. Considering the encouraging outcomes, subsequent studies ought to investigate the capabilities of multi-axis tracking systems and artificial intelligence-based optimization to further improve solar energy collection and system sustainability.

REFERENCES

Alsheekh, M., Najim, S. E., and Sultan, H. S. (2021). Experimental, Theoretical, and CFD Validations for Solar-Powered Atmospheric Water Generation Using Thermoelectric Techniques. Basrah Journal for Engineering Sciences, 21(2).

Chen, R., and Zhang, J. S. (2014). Half Load-Cycle Worked Dual Input Single Output DC/AC Inverter. Journal of Power Electronics, 14(6), 1217–1223.

Firth, S., Lomas, K. and Rees, S. (2010). A Simple Model of PV System Performance and Its Use in Fault Detection. Solar Energy, 4(84), 624-635.

García-Rodríguez, V. H., Pérez-Cruz, J. H., Ambrosio-Lázaro, R. C., and Tavera-Mosqueda, S. (2023). Analysis of DC/DC Boost Converter–Full-Bridge Buck Inverter System for AC Generation. Energies, 16(6), 2509.

Hammadi, S. H., and Mohammed, A. H. (2014). Application of earth tube heat exchanger and solar chimney for natural cooling system in Basrah City. Journal for Engineering Sciences, 23-32.

Hao, X., Shan, S., Gao, N., Chen, G., Wang, Q., and Gu, T. (2023). Performance analysis of a novel combined cooling, heating, and power system with solar energy spectral beam splitting. *Energy Conversion and Management*, *276*, 116500.

Hellström, B. (2004). Derivation of efficiency factors for uneven irradiation on a fin absorber. Solar Energy, 77(3), 261–267.

Jeykishan K., K., Sudhir Kumar, R., and Bhattacharjee, T. (2021). An alternate method for evaluating power-temperature derating characteristics of grid-tyed solar photovoltaic inverters. Sādhanā, 46(3).

Kaplan, E. (2012). Detection of Degradation Effects in Field-aged C-si Solar Cells through Ir Thermography and Digital Image Processing. International Journal of Photoenergy, (2012), 1-11.

Mathew, D., Rani, C., Kumar, M., Wang, Y., Binns, R., and Busawon, K. (2018). Wind-driven Optimization Technique for Estimation of Solar Photovoltaic Parameters. IEEE J. Photovoltaics, 1(8), 248-256.

Meng, Z., and Chen, L. (2020). Theoretical maximum efficiency and higher power output in triboelectric nanogenerators. Energy Reports, 6, 2463–2475.

Photocatalytic efficiency of titania nonylphenol ethoxylate composite thin films under solar irradiation. (2022). Focus on Surfactants, 2022(1), https://doi.org/10.1016/j.fos.2021.12.010

Sangotayo, E. O., Itabiyi, O. E., Mudashiru, L. O., Oyeniran, N. D, and Jalekun, O. I, (2018) Thermal Effect of Photovoltaic Hybrid Solar Cells on Electrical Efficiency of Solar Inverter, Adeleke University Journal of Engineering and Technology [AUJET], 1(1), 184-195,

Serban, E., Pondiche, C., and Ordonez, M. (2019). Modulation Effects on Power-Loss and Leakage Current in Three-Phase Solar Inverters. IEEE Transactions on Energy Conversion, 34(1), 339–350.

Shittu, S., Li, G., Zhao, X., Akhlaghi, Y., Ma, X., and Yu, M. (2019). Comparative Study of a Concentrated Photovoltaic-Thermoelectric System with and without Flat Plate Heat Pipe. Energy Conversion and Management, (193), 1-14.

Stropnik, R. and Stritih, U. (2016). Increasing the Efficiency of PV Panel with the Use of Pcm. Renewable Energy, (97), 671-679.